

# Physicochemical characterization of the retardation of aqueous Cs<sup>+</sup> ions by natural kaolinite and clinoptilolite minerals

T. Shahwan\*, D. Akar, A.E. Eroğlu

*Department of Chemistry, Izmir Institute of Technology, Urla 35430, Izmir, Turkey*

Received 12 July 2004; accepted 3 November 2004

## Abstract

The aim of this study was to carry out kinetic, thermodynamic, and surface characterization of the sorption of Cs<sup>+</sup> ions on natural minerals of kaolinite and clinoptilolite. The results showed that sorption followed pseudo-second-order kinetics. The activation energies were 9.5 and 13.9 kJ/mol for Cs<sup>+</sup> sorption on kaolinite and clinoptilolite, respectively. Experiments performed at four different initial concentrations of the ion revealed that the percentage sorption of Cs<sup>+</sup> on clinoptilolite ranged from 90 to 95, compared to 28 to 40 for the kaolinite case. At the end of a 1 week period, the percentage of Cs<sup>+</sup> desorption from clinoptilolite did not exceed 7%, while it amounted to more than 30% in kaolinite, indicating more stable fixation by clinoptilolite. The sorption data were best described using Freundlich and D–R isotherm models. Sorption showed spontaneous and exothermic behavior on both minerals, with  $\Delta H^0$  being  $-6.3$  and  $-11.4$  kJ/mol for Cs<sup>+</sup> uptake by kaolinite and clinoptilolite, respectively. Expanding the kaolinite interlayer space from 0.71 to 1.12 nm using DMSO intercalation, did not yield a significant enhancement in the sorption capacity of kaolinite, indicating that the surface and edge sites of the clay are more energetically favored. EDS mapping and elemental analysis of the surface of kaolinite and clinoptilolite revealed more intense signals on the surface of the latter with an even distribution of sorbed Cs<sup>+</sup> onto the surfaces of both minerals.

© 2004 Elsevier Inc. All rights reserved.

**Keywords:** Kaolinite; Clinoptilolite; Cs<sup>+</sup>; Sorption

## 1. Introduction

The reliable prediction of metal transport through the biological environment requires a thorough knowledge of the parameters which influence their migration behavior. Those parameters are mostly related with the properties of liquid and solid phases in contact. Among the properties of the liquid phase are the time of contact, pH,  $E_h$ , loading, ionic strength, and temperature. The properties of the solid phase, however, are determined by factors such as the cation exchange capacity and the particle size, which are closely related to the structural features of these solids.

Cesium, Cs, is an alkali element ( $Z = 55$ ) that has high solubility in water. It possesses several radioactive

isotopes, the most important of which are  $^{134}\text{Cs}$  ( $t_{1/2} = 2.06$  years),  $^{135}\text{Cs}$  ( $t_{1/2} = 3.0 \times 10^6$  years), and  $^{137}\text{Cs}$  ( $t_{1/2} = 30.17$  years) produced during nuclear fission processes. The fission yields of  $^{135}\text{Cs}$  and  $^{137}\text{Cs}$  are relatively high, 6.54 and 6.18%, respectively [1]. Due to their long half lives, both of  $^{135}\text{Cs}$  and  $^{137}\text{Cs}$  are principal radiocontaminants. The Cs<sup>+</sup> ion can be highly mobile in aqueous media due to its low hydration energy ( $-276$  kJ/mol) as compared to elements of larger oxidation state or smaller size, for which the hydration energies can rise up to several thousands of kilojoules per mole. This property facilitates its involvement with the hydrological cycle, which has interfaces with the biological cycle and thus poses a potential detriment to man and to other living systems.

Kaolinite and clinoptilolite are two examples of aluminosilicates that are widely available as soil components. The difference in structural properties of these two minerals af-

\* Corresponding author. Fax: +90-232-750-7509.

E-mail address: [talalshahwan@iyte.edu.tr](mailto:talalshahwan@iyte.edu.tr) (T. Shahwan).

fects their retardation behavior of different metals. Kaolinite is a 1:1 clay mineral that possesses a tight interlayer structure with the ideal formula  $\text{Al}_2\text{Si}_2\text{O}_5(\text{OH})_4$  [2]. The sorption properties of this clay are solely determined by the nature of its surface and edges. Kaolinite possesses a variable charge that can be related to the reactions between ionizable surface groups located at the edges or at the gibbsite basal plane and the ions present in aqueous solution [3]. The same study showed that the silanol groups ( $\text{Si}-\text{OH}$ ) at the crystal edges of kaolinite contribute exclusively to the negative charge, through formation of  $\text{SiO}^-$  surface complexes at moderate and high pH values. The aluminol groups at the edges are amphoteric; undergoing protonation at low pH and deprotonation at high pH, resulting in the formation of the surface complexes  $\text{AlOH}_2^+$  and  $\text{AlO}^-$ . It is also stated by another study that the charge from broken edges and exposed OH planes rather than charge from Al/Si substitution determines the kaolinite CEC, even at zero point charge, and that a high CEC in some kaolinites is found to be due to smectite layers on the surface of the kaolinite crystals [4]. However, it is indicated by other researches that the negative charge on kaolinite cannot be attributed to an oxide-like source only, and the partial dissolution of structural aluminum yielding negatively charged vacant sites must also be considered [5].

Clinoptilolite is one of the most widely known zeolitic minerals. The sorption on zeolitic particles is a complex process because of their porous structure, inner and outer charged surfaces, mineralogical heterogeneity, existence of crystal edges, broken bonds, and other imperfections on the surface [6]. The elemental formula of clinoptilolite is  $(\text{Na,K})_6\text{Al}_6(\text{Si}_{30}\text{O}_{72})\cdot 20\text{H}_2\text{O}$  [7]. The cage-like structure of this mineral makes it suitable for ion exchange reactions. In the absence of steric factors that can stabilize the ions held within the cages, such a stabilization might be referred to the negative charge arising from the isomorphous substitution of  $\text{Al}^{3+}$  with  $\text{Si}^{4+}$  in the structure. Another factor could also be the deprotonation of the oxide groups if the operational pH of the medium exceeds the zero point of charge of clinoptilolite. It is also reported that the sorbed cations might be coordinated with the defined number of water molecules, and located on specific sites in framework channels [6]. Clinoptilolite has received extensive attention due to its attractive selectivity for certain heavy metal cations such as lead, cadmium, and nickel [8].

So far, a variety of studies have been devoted to characterizing various aspects of the sorption behavior of  $\text{Cs}^+$  ion on kaolinite and on clinoptilolite, using a variety of characterization techniques [9–18]. In our earlier studies, the retention capacity of kaolinite toward  $\text{Cs}^+$  was studied and compared with that of other clay minerals [9]. A depth profiling study was also carried out to reveal the distribution of  $\text{Cs}^+$  across the surface of kaolinite [10]. The applicability of kaolinite as a reactive barrier for  $\text{Cs}^+$  retention was tested by other authors and the irreversibility of its uptake by kaolinite was discussed and compared with other clay minerals [11,12]. The sorption sites and atomic dynamics of  $\text{Cs}^+$  on kaolin-

ite were investigated and compared with its uptake by illite and montmorillonite [13,14]. The effectiveness of clinoptilolite as countermeasure amendments against  $\text{Cs}^+$  migration from soil into plants was reported [15]. In another study, it was documented that the addition of clinoptilolite to cements leads to a 70–75% decrease in  $\text{Cs}^+$  release [16].

In this study, the sorption behavior of  $\text{Cs}^+$  on natural samples dominated by kaolinite and clinoptilolite was investigated as a function of contact time, loading, and temperature using atomic absorption spectroscopy (AAS), scanning electron microscopy–energy dispersive X-ray spectroscopy (SEM–EDS), and X-ray powder diffraction (XRPD). The study aimed at determination of the sorption kinetics, the best fitting isotherm model(s), and thermodynamic parameters such as the activation energy, enthalpy change, entropy change, and Gibbs energy of sorption, in addition to elucidating the surface distribution of the sorbed  $\text{Cs}^+$  using elemental and mapping analysis of EDS technique.

## 2. Experimental

Natural samples of kaolinite and clinoptilolite used in this study originated from the Sındırgı and Manisa regions located in the western part of Anatolia. The samples were dry-sieved and the particle size of kaolinite used in this study was  $<38\ \mu\text{m}$ , while that of clinoptilolite was 75–150  $\mu\text{m}$ . Prior to performing the sorption steps, the mineral samples were equilibrated with tap water. The pretreatment step aimed to mimic the equilibrium situation of the minerals with groundwater. In each batch of the pretreatment experiments, 10.0 g of the mineral and 1000 ml of laboratory tapwater were mixed on a lateral shaker at room temperature for 4 days. The mineral samples were then filtered and dried.

The sorption experiments were performed using 50-ml polyethylene tubes. The tubes were first cleaned, dried at 90 °C overnight, cooled, and weighed. To each tube, 0.50 g of kaolinite or clinoptilolite samples were added, followed by the addition of 50.0 ml of aqueous  $\text{CsCl}$  solution. The initial concentrations of the solutions were 10, 50, 100, and 500 mg/l. The mixtures were then mixed using a Nuve ST 402 water bath shaker equipped with a microprocessor thermostat. The experiments were carried out at 25 and 60 °C for contact periods of 5, 10, and 30 min, and 1, 2, 5, 8, 24, and 48 h. At the end of each mixing period, the samples were filtered and dried at 90 °C. The filtrate was then analyzed using flame AAS using a Thermo Elemental SOLAAR M6 Series atomic absorption spectrometer with air–acetylene flame. A Cs hollow-cathode lamp ( $\lambda = 758.0\ \text{nm}$ ) was applied as a source.

In the desorption experiments, samples of Cs-loaded kaolinite and Cs-loaded clinoptilolite, prepared previously after 48 h of mixing, were exposed to tap water and shaken for a time period that lasted for one week. Analysis of the eluted  $\text{Cs}^+$  were performed at 10 min, 4 h, 24 h, and 7 days.

The concentration of the eluted Cs was then measured using AAS.

The intercalation of dimethylsulfoxide (DMSO) within the kaolinite lamellae was achieved by stirring a suspension composed of 20 g of the clay in 100 ml DMSO for 24 h at 65 °C. The redundant DMSO was then removed by sedimentation, repeated washes with methanol, and decanting over a period of 5 days [19].

XRPD analysis of the mineral phases was performed using a Philips X'Pert Pro diffractometer located at Center of Materials Research/Izmir Institute of Technology and a Rigaku Miniflex X-ray diffractometer located at Department of Chemistry/Bilkent University. The samples were first ground, mounted on holders then introduced for analysis. The source consisted of  $\text{CuK}\alpha$  radiation ( $\lambda = 1.54 \text{ \AA}$ ). Each sample was scanned within the  $2\theta$  range 2–60. The step size was 0.020 with a time per step duration of 60 s.

SEM/EDS characterization was carried out using a Philips XL-30S FEG type instrument. Prior to analysis, the solid samples were sprinkled onto adhesive carbon taps supported on metallic disks. Images of the sample surfaces were recorded at different magnifications with the highest being  $\times 80,000$ . EDS elemental analysis was performed at different points on the surface in order to minimize any possible anomalies arising from the heterogeneous nature of the analyzed surface. EDS mapping was conducted at magnification

of  $\times 500$  and a voltage of 18 kV under vacuum conditions of  $3.5 \times 10^{-5}$  mbar.

### 3. Results and discussion

Natural samples of kaolinite and clinoptilolite were analyzed for their mineral constituents using XRPD and for their elemental contents using EDS. As shown in Fig. 1a, natural kaolinite contains quartz as an impurity. According to the Fig. 1b, clinoptilolite seems to be almost pure. SEM analysis indicated that kaolinite has a well-defined crystal structure as seen from the characteristic hexagonal morphology with edge sizes ranging from 300 to 500 nm as given in Fig. 1c. Clinoptilolite, however, seems to be composed of crystals with varying shape and nondefinite morphology and size that amounts to several micrometers as shown by Fig. 1d. The EDS results showed that the average elemental content of kaolinite was 66.8% O, 17.6% Si, and 14.1% Al, in addition to minor quantities of Na, K, Mg, and Ca probably originating from a smectitic-like clay impurity that is below the detection limit of XRPD. The average elemental content of clinoptilolite was 61.9% O, 23.7% Si, and 5.3% Al, including small amounts of Na, K, Mg, and Ca. These values represent an average of five data points obtained from random locations on the mineral surface.

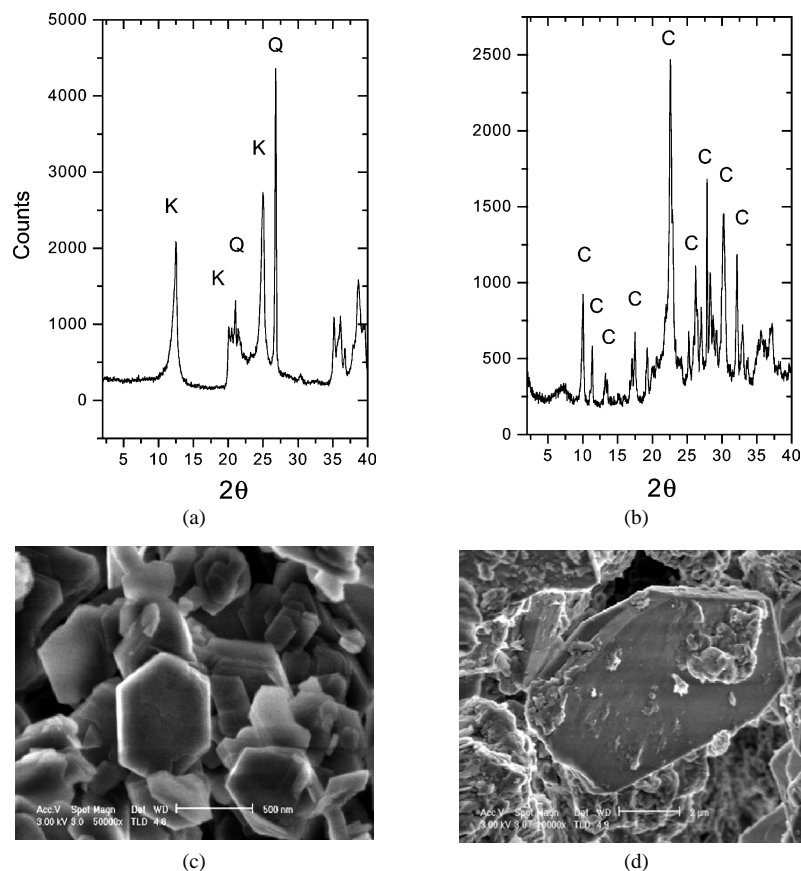


Fig. 1. (a) XRPD diagram of natural kaolinite, (b) XRPD diagram of natural clinoptilolite, (c) a typical SEM microimage of natural kaolinite, and (d) a typical SEM microimage of natural clinoptilolite; (K) kaolinite, (Q) quartz, (C) clinoptilolite.

### 3.1. Kinetic analysis

The sorption studies carried out as a function of contact time for different initial concentrations indicated that at the initial concentrations of 10, 50, and 100 mg/l, equilibrium of sorbed  $\text{Cs}^+$  was achieved within 10 min on both minerals at temperatures of 25 and 60 °C. The percentage sorption at these concentrations ranged between 29 and 40 in the case of kaolinite, and 90 and 95 in the case of clinoptilolite. As the initial concentration of  $\text{CsCl}$  solutions was raised to 500 mg/l, the time required to reach equilibrium in the case of  $\text{Cs}^+$  sorption on kaolinite increased to about 500–1000 min, as shown in Fig. 2a. The data indicate fast accumulation of the ions at the kaolinite surface followed by a partial desorption leading to equilibrium attainment. A sorption reaction is believed to pass through three steps [20]: film diffusion, particle diffusion, and finally the exchange reaction at the sorption site. The behavior reported above might indicate that at higher loadings of  $\text{Cs}^+$ , intrinsic sorption (or exchange reaction) on kaolinite sites becomes slower than the rate of transfer of  $\text{Cs}^+$  ions from the bulk to the sorption layer, the thing probably stemming from the competition between the sorbate ions towards the limited number of sorption sites on kaolinite. In the case of clinoptilolite, however, equilibrium seemed to be achieved at longer times, as shown in Fig. 2b. The data suggest that, unlike the kaolinite case, intrinsic sorption seems to be faster than bulk and pore diffusion. Upon increasing the operating temperature to 60 °C, no significant change was observed in

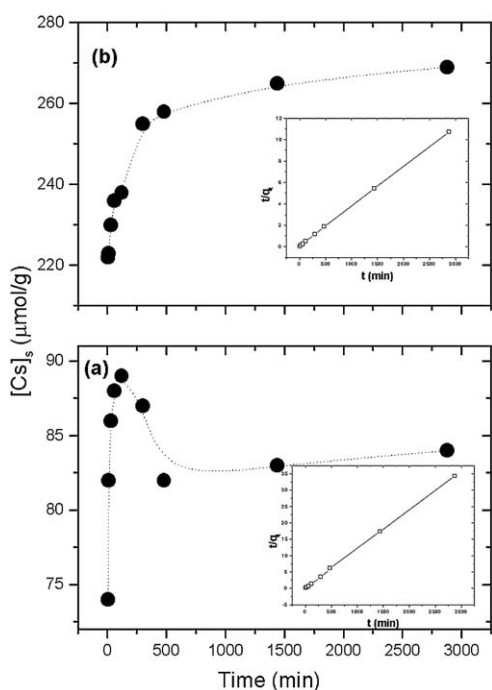


Fig. 2. (a) Variation of the sorbed amount of  $\text{Cs}^+$  ( $\mu\text{mol/g}$ ) on kaolinite with time; (b) variation of the sorbed amount of  $\text{Cs}^+$  ( $\mu\text{mol/g}$ ) on clinoptilolite with time. The insets in both figures give the corresponding linear fits using the pseudo-second-order equation.

the kinetic behavior of  $\text{Cs}^+$  reported above for both minerals.

In order to calculate the “apparent” rate constant, the following pseudo-first-order equation [21] and pseudo-second-order equation [22] were used,

$$\frac{1}{[C]_s} = \left( \frac{k_1}{[C]_e} \right) \left( \frac{1}{t} \right) + \frac{1}{[C]_e}, \quad (1)$$

$$\frac{t}{[C]_s} = \left( \frac{1}{k_2[C]_e^2} \right) + \left( \frac{1}{[C]_e} \right) t, \quad (2)$$

where  $[C]_s$  is the concentration of  $\text{Cs}^+$  sorbed on the solid at time  $t$  ( $\mu\text{mol/g}$ ),  $[C]_e$  is the concentration of  $\text{Cs}^+$  sorbed at equilibrium,  $k_1$  is the pseudo-first-order rate constant ( $1/\text{min}$ ), and  $k_2$  is the pseudo-second-order rate constant ( $\text{g}/\mu\text{mol min}$ ). The concentration on the solid,  $[C]_s$ , was calculated using the equation

$$[C]_s = ([C]_0 - [C]_l)(V/M). \quad (3)$$

Here  $[C]_0$  is the initial concentration ( $\mu\text{mol/l}$ ),  $[C]_l$  is the concentration in the liquid at time  $t$  ( $\mu\text{mol/l}$ ),  $V$  is the volume of the solution (l), and  $M$  is the mass of the solid (g). Plots obtained using Eq. (1) indicated that the sorption of  $\text{Cs}^+$  on both of kaolinite and clinoptilolite did not follow the pseudo-first-order kinetics at any concentration or temperature. Applying Eq. (2), however, leads to linear fits with correlation coefficient close to unity. Although our data show almost a perfect correlation with Eq. (2), we would like to stress that, in our opinion, an important limitation on the applicability of this equation is that the equation would lead to perfect linearity (linear correlation coefficient of 1.0) even if the sorbed amount did not show any variation with time. Moreover, there is a possibility of obtaining a negative intercept (implying that the rate constant possesses a negative value) even in a case where the linear correlation coefficient might be 1.0. Due to this, we have chosen to apply the equation for the sorption data at initial concentration of  $\text{CsCl}$  of 500 mg/l only, the concentration at which the uptake by the solids showed a gradual increase with time leading to equilibrium. The insets in Fig. 2a and Fig. 2b show the change in  $t/q_t$  versus  $t$ . The values of the linear correlation coefficients,  $k_2$ , and  $[C]_e$  obtained at this initial concentration and temperatures of 25 and 60 °C are shown in Table 1. The same table gives also the activation energy of sorption ( $E_a$ ; kJ/mol) calculated using the equation

$$\ln \frac{k_2(T_2)}{k_2(T_1)} = -\frac{E_a}{R} \left( \frac{1}{T_2} - \frac{1}{T_1} \right). \quad (4)$$

Here  $R$  is the perfect gas constant (8.314 J/mol K). The values of  $E_a$  were obtained as 9.5 and 13.9 kJ/mol for the sorption of  $\text{Cs}^+$  on kaolinite and clinoptilolite, respectively. The activation energy can be conceived as the minimum kinetic energy required for a given reaction to take place. The values of  $E_a$  thus indicate that the energetic barrier against sorption on kaolinite is easier to overcome compared to that on clinoptilolite, the thing that might contribute to a faster

Table 1

The values of  $k_2$  and  $[C]_e$  obtained from the linear fits of the experimental data to the second-order rate equation

Sample	$T$ (°C)	$[C]_e$ ( $\mu\text{mol/g}$ )	$k_2$ ( $\text{g}/\mu\text{mol min}$ )	$R$	$E_a$ (kJ/mol)
Cs-loaded clinoptilolite	25	270	$3.5 \times 10^{-4}$	0.9997	13.9
Cs-loaded clinoptilolite	60	261	$6.4 \times 10^{-4}$	0.9996	
Cs-loaded kaolinite	25	84	$7.2 \times 10^{-3}$	0.9999	9.5
Cs-loaded kaolinite	60	87	$1.1 \times 10^{-2}$	0.9998	

Note. The table also gives the linear correlation coefficients,  $R$ , and the activation energy,  $E_a$ , corresponding to  $\text{Cs}^+$  uptake by kaolinite and clinoptilolite minerals.

sorption on the former. In both cases, the  $E_a$  values are much below the energies corresponding to chemisorption barriers (usually  $>40$  kJ/mol), suggesting that physical sorption is operating where the attractive forces are of van der Waals type in addition to weak electrostatic forces accompanying most ion-exchange reactions.

As given in Table 1, the  $k_2$  values indicate that the sorption on kaolinite is faster than on clinoptilolite, the thing probably related to the fact that the sorption sites on kaolinite are located mainly on the “more easily” accessible surface and edge locations. This means that it would be enough for  $\text{Cs}^+$  ions to overcome the film diffusion barrier to reach the sorption layer (although the following step of intrinsic sorption might be slow, as discussed previously). In the clinoptilolite case, however, in addition to surface sites, the sorption sites inside the channels of the mineral might be operative, thus  $\text{Cs}^+$  ions are required to additionally overcome the pore diffusion barrier before reaching the internal sorption sites, in particular when loading is increased to the limit that necessitates an increasing involvement of the internal sites. The effect of intraparticle diffusion on sorption was tested using the equation [21]

$$[C]_s = k_p t^{1/2} + C. \quad (5)$$

In this equation,  $k_p$  corresponds to the intraparticle diffusion rate constant ( $\text{g}/\mu\text{mol min}$ ), and  $C$  is a constant related to the boundary layer thickness. A plot of Eq. (5) for  $\text{Cs}^+$  sorption indicated that while in the kaolinite case no linear behavior was observed over the studied time periods, a linear relation was observed for  $\text{Cs}^+$  sorption on clinoptilolite at the initial stages of sorption ( $t < \sim 100$  min), followed by a curved portion leading to a plateau, as shown in Fig. 3. This suggests that intraparticle diffusion affects the rate at the initial stages of sorption, but it is not the rate-determining step. It is reported that intraparticle diffusion can be considered to be the rate-determining step if the obtained straight line that passes through the origin is obtained upon plotting  $[C]_s$  versus  $t^{1/2}$  [23]. The linear portions in Fig. 3 yield  $k_p$  values of 1.99 and 2.47  $\text{g}/\mu\text{mol min}$  for  $\text{Cs}^+$  sorption on clinoptilolite at 25 and 60 °C, respectively. It is important to note that the presence of internal sites in clinoptilolite is believed to be responsible for the higher sorption capacity of this mineral. This can be validated from the much higher percentage

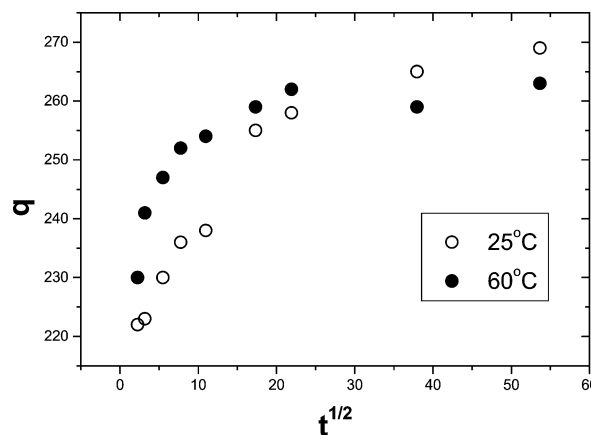


Fig. 3. Intraparticle diffusion plots of sorbed  $\text{Cs}^+$  on clinoptilolite at 25 and 60 °C.

sorption of clinoptilolite compared to kaolinite given previously.

In order to check the sorption stability of  $\text{Cs}^+$  ions fixed by kaolinite and clinoptilolite, desorption experiments were performed. Samples prepared initially by sorption experiments with initial concentrations of  $\text{CsCl}$  of 10 and 50  $\text{mg/l}$ , were contacted with tap water (which was used in the pre-treatment step of kaolinite and clinoptilolite) and shaken for periods ranging from 4 h up to 7 days at controlled temperatures of 25 and 60 °C. The results indicated that in the case of kaolinite the percentage desorption ranged between 30 and 39. In the case of clinoptilolite, however, the percentage desorption ranged between 4 and 7, indicating a more stable fixation. In both cases, almost the whole desorbed amounts were released within the first 4-h period. It is reported that the  $\text{Cs}^+$ -preloaded kaolinite samples can release  $\text{Cs}^+$  more readily than  $\text{Cs}^+$ -preloaded illite can do and that appropriate concentrations of alkylammonium salts would lead to 80% desorption of the  $\text{Cs}^+$  initially uploaded on kaolinite [12].

### 3.2. Isotherms

The sorption data obeyed both of Freundlich and Dubinin–Radushkevich isotherm models. Freundlich isotherm model is an empirical equation that describes adsorption on solids with sites that might vary in their sorption energy, without any restriction on the sorption capacity of those solids. This isotherm model is given as

$$[C]_s = k[C]_l^n. \quad (6)$$

Here  $[C]_s$  corresponds to the equilibrium concentration of the sorbate on the solid ( $\text{meq/ml}$ ),  $[C]_l$  is the equilibrium concentration of  $C$  in the liquid phase at time  $t$ ,  $k$  is the Freundlich constant, and  $n$  is a measure of sorption linearity. Plots of the sorption data corresponding to mixing periods of 48 h at temperatures of 25 and 60 °C for sorption of  $\text{Cs}^+$  on kaolinite and clinoptilolite are given in Fig. 4. The corresponding values of Freundlich constants are given in Table 2. In terms of sorption linearity, the values of  $n$  are

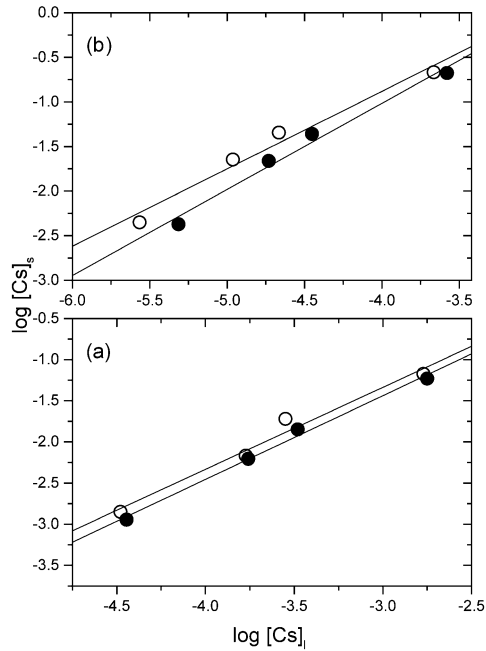


Fig. 4. Freundlich isotherm model plots of (a)  $\text{Cs}^+$  sorbed by kaolinite and (b)  $\text{Cs}^+$  sorbed by clinoptilolite at  $T = 25^\circ\text{C}$  (○) and  $T = 60^\circ\text{C}$  (●).

closer to unity in the case of kaolinite compared to clinoptilolite, the thing that is indicative of more homogeneity of the sorption sites of the former. The  $k$  values in the case of clinoptilolite are much larger than those corresponding to kaolinite, the thing reflecting the larger affinity of clinoptilolite towards  $\text{Cs}^+$  sorption. Temperature is observed to have a more prominent effect on the sorption affinity of clinoptilolite compared to kaolinite.

The Dubinin–Radushkevich isotherm model is given by the equation

$$[C]_s = C_m \exp(K\varepsilon^2), \quad (7)$$

where  $\varepsilon$  is given as  $RT \ln(1 + 1/[C]_l)$ ,  $R$  is the ideal gas constant (8.3145 J/molK),  $T$  is the absolute temperature (K),  $K$  is a constant related to sorption energy, and  $C_m$  refers to the sorption capacity of adsorbent per unit weight (meq/g).  $K$  and  $C_m$  are obtained from the least-square fits of the sorption data constructed using the linearized form of Eq. (7). Fig. 5 gives plots of the data corresponding to a contact period of 48 h and temperatures of 25 and 60 °C. The sorption energy,  $E$ , can be calculated using  $K$  values from the rela-

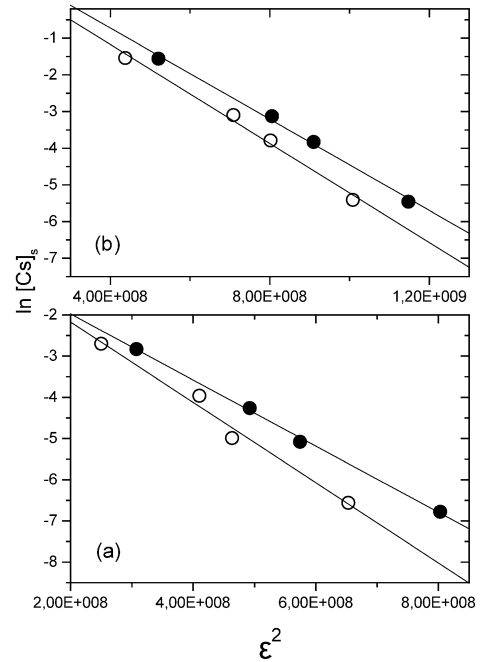


Fig. 5. Dubinin–Radushkevich isotherm plots of (a)  $\text{Cs}^+$  sorbed by kaolinite and (b)  $\text{Cs}^+$  sorbed by clinoptilolite at  $T = 25^\circ\text{C}$  (○) and  $T = 60^\circ\text{C}$  (●).

tion

$$E = (-2K)^{-0.5}. \quad (8)$$

Here  $E$  refers to the amount of energy required to transfer one mole of sorbed ions from infinity in solution to the solid surface. The values of  $C_m$ ,  $K$ , and  $E$  are given in Table 2. Again it is evident from the values of  $C_m$  that clinoptilolite possesses a larger sorption capacity than kaolinite, and that relatively weak forces of interaction exists between the sorbed  $\text{Cs}^+$  ions and the sorbent sites, as indicated by the values of  $E$ , which lie much below the typical values corresponding to some sort of chemical bonding.

### 3.3. Thermodynamic parameters

Evaluation of thermodynamic parameters such as  $\Delta H^0$  and  $\Delta G^0$  necessitates first the definition of an equilibrium constant that is valid over a given concentration range. An important difficulty associated with the description of sorption data is the lack of an equilibrium constant that might be used to describe the relation between the equilibrium amount

Table 2

The values of  $n$  and  $k$  obtained from the Freundlich isotherm model and the values of  $K$ ,  $C_m$ , and  $E$  obtained from the Dubinin–Radushkevich isotherm model for  $\text{Cs}^+$  uptake by kaolinite and clinoptilolite minerals

Sample	$T$ ( $^\circ\text{C}$ )	Freundlich isotherm			Dubinin–Radushkevich isotherm			
		$n$	$k$	$R$	$K$	$C_m$ (meq/100 g)	$E$ (kJ/mol)	$R$
Cs-loaded kaolinite	25	0.99	45	0.9980	0.0098	0.80	7.1	0.9991
	60	1.00	41	0.9973	0.0080	0.69	7.9	0.9924
Cs-loaded clinoptilolite	25	0.96	692	0.9921	0.0062	5.81	9.0	0.9960
	60	0.87	389	0.9880	0.0068	4.57	8.6	0.9980

Table 3

The  $R_d$  values (ml/g) corresponding to sorption of  $\text{Cs}^+$  on kaolinite and clinoptilolite at temperature of 25 and 60 °C at various initial concentrations and a mixing period of 48 h

[C] <sub>0</sub> of CsCl (mg/l)	Cs-loaded kaolinite		Cs-loaded clinoptilolite	
	25 °C	60 °C	25 °C	60 °C
500	40	33	993	798
100	68	43	2093	1239
50	40	36	2071	1174
10	43	32	1640	875

of a sorbed species on the solid phase to that in the liquid phase over a wide range of concentrations. Usually, this difficulty is partially foiled through applying empirical distribution constants,  $R_d$  (ml/g), defined as

$$R_d = \frac{[C]_s}{[C]_l} \quad (9)$$

Each of the  $R_d$  values is valid at a particular initial concentration and reaction conditions. The  $R_d$  values corresponding to sorption of  $\text{Cs}^+$  on kaolinite and clinoptilolite at temperatures of 25 and 60 °C at various initial concentrations and a mixing period of 48 h are given in Table 3. It might be interesting to note the  $R_d$  values of  $\text{Cs}^+$  sorption on kaolinite obtained in this study using AAS measurements are close the values that we have obtained in an earlier study performed using the radiotracer method [9].

The  $R_d$  values were used in the calculation of the enthalpy change of sorption,  $\Delta H^0$ , and the Gibbs energy of sorption,  $\Delta G^0$ , by applying the equations

$$\Delta H^0 = R \ln \frac{R_d(T_2)}{R_d(T_1)} \left( \frac{1}{T_1} - \frac{1}{T_2} \right)^{-1} \quad (10)$$

$$\Delta G^0 = -RT \ln R_d \quad (11)$$

Table 4 gives the values of  $\Delta H^0$  and  $\Delta G^0$  obtained using the above equations after they were averaged over the entire concentration range. The sorption in both cases comes

Table 4

$\Delta H^0$  and  $\Delta G^0$  values calculated from the sorption data of  $\text{Cs}^+$  on kaolinite and clinoptilolite minerals

Sample	$\Delta H^0$ (kJ/mol)	$\Delta G^0$ (kJ/mol)	
		298 K	333 K
Cs-loaded kaolinite	-6.3	-9.6	-9.9
Cs-loaded clinoptilolite	-11.4	-18.4	-19.2

out to be exothermic and spontaneous, indicating that lower temperatures are favored. The reason for this behavior could originate from thermal destabilization leading to an increase of the mobility of the  $\text{Cs}^+$  on the surface of the solid as the operating temperature is increased, thus enhancing the desorption steps. The parallel increase in the  $\text{Cs}^+$  mobility within the solution—which could make a positive contribution to sorption—is expected to be insignificant because the ion already possesses a high mobility due to the weak hydration forces of water molecules the thing caused by the low charge density (charge/size) of  $\text{Cs}^+$  ions. The values obtained for the kaolinite case are close to our earlier findings obtained using the radiotracer technique over a wider range of concentration [9]. For both minerals, the obtained results are within the energy range 8–16 kJ/mol, which corresponds to ion-exchange-type sorption mechanism [24].

#### 4. EDS characterization

Spot analysis of the Cs-sorbed kaolinite and clinoptilolite was performed at 10 different positions selected randomly on the surfaces of the minerals. This analysis was also supported by EDS mapping of mineral surfaces. The EDS mapping microimages for the elements Al, Si, and Cs are given in Fig. 6. The figure indicates that Cs is distributed across the surfaces of both minerals with no apparent localization. The signals of the Cs on clinoptilolite appears to be more intense

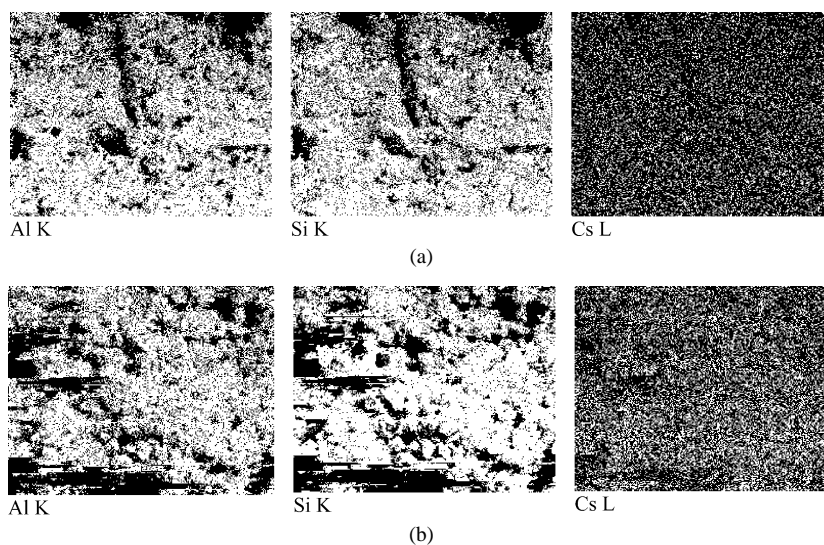


Fig. 6. EDS mapping images showing the distribution of elements Al, Si, and Cs on the surfaces of (a) Cs-loaded kaolinite and (b) Cs-loaded clinoptilolite.

Table 5

EDS findings of the atomic percentages of O, Si, Al, and Cs in Cs-loaded kaolinite and clinoptilolite minerals obtained from spot analysis at 10 different points selected randomly on the surfaces of the minerals

Spot No.	Cs kaolinite				Cs-clinoptilolite			
	O	Si	Al	Cs	O	Si	Al	Cs
1	63.14	16.23	14.13	0.23	61.24	23.59	5.32	0.65
2	63.90	16.82	13.11	0.13	61.88	22.75	5.11	0.77
3	65.53	13.55	13.48	0.12	60.44	23.95	5.05	0.68
4	66.02	13.94	12.98	0.05	61.20	23.35	5.34	0.79
5	63.20	16.05	13.02	0.13	61.73	22.86	5.14	0.76
6	65.79	13.85	12.89	0.07	60.81	22.92	5.17	0.77
7	65.72	16.22	11.57	0.17	61.16	23.60	5.35	0.70
8	64.98	14.59	14.24	0.14	60.75	23.71	5.50	0.91
9	64.11	14.29	14.86	0.17	60.75	23.53	5.68	0.95
10	64.66	14.27	13.94	0.14	62.42	21.75	5.29	0.69
Mean	64.71	14.98	13.42	0.14	61.24	23.20	5.30	0.77
S.D.	1.08	1.21	0.92	0.05	0.61	0.65	0.19	0.10

Note. S.D.: standard deviation.

than those on kaolinite. The results of the EDS spot elemental analysis of O (*K* line), Si (*K* line), Al (*K* line), and Cs (*L* line) are given in Table 5. The higher uptake capacity of clinoptilolite is evident from the higher atomic percentage (approximately five times larger) compared with kaolinite. The Cs signal, as well as those of Al and Si, are showing higher variation with location compared to clinoptilolite, the thing that might be referred to the higher heterogeneity of the natural kaolinite sample compared to clinoptilolite (which was discussed previously). It must be stressed that these data correspond to a depth analysis of around 2  $\mu\text{m}$  from the upper surface and that for elements with amounts of less than 1%, the percentage error in the EDS signal might exceed 50 (as indicated by the manufacturer of the instrument; EDAX).

## 5. XRPD analysis of the Cs-loaded minerals

The XRPD of the Cs-loaded kaolinite and clinoptilolite samples revealed no meaningful change in the shape or positions of the features provided by Figs. 1a and 1b. Some minor intensity variations were, however, obtained the thing stemming primarily from grain size orientation of the powder samples. This problem is usually foiled by multiple preparation and measurement of each sample. These findings indicate no change in the lattices of the minerals upon uptake of  $\text{Cs}^+$  ions. Structural stability of clinoptilolite is not expected to be affected by uptake of cations, especially if this uptake takes place near the neutral pH range, as was the case in our experiments. It is reported that this mineral can even withstand acidic attack up to a pH around 1 [8]. As was discussed earlier, the sorption sites of kaolinite are located mainly on the surface and edge parts [3]; thus the basal (interlayer) space is expected to retain its dimensions upon sorption. Nevertheless, it is reported that incorporation of foreign ions within the kaolinite structure would bring about a stress on the kaolinite molecule, the

thing that might influence properties such as swelling capacity, compaction capability, and the double-layer behavior of the clay [25].

To check the effect of interlayer expansion on the uptake capacity of kaolinite, the clay was intercalated with dimethylsulfoxide, DMSO to overcome the tight H-bonding interconnecting the layers of the clay. XRPD characterization showed that upon such modification, the 001 and 002 reflections of the clay changed from 0.71 and 0.35 nm to 1.12 and 0.37 nm, respectively. Upon exposure of the DMSO-intercalated kaolinite to  $\text{Cs}^+$ , the original reflections evolved again, but with smaller intensities. The data showed that, as a result of expanding the interlayer space of kaolinite, the percentage sorption of  $\text{Cs}^+$ , with initial concentrations of CsCl of 100 and 500 mg/l, increased slightly from 31 to 37 and from 28 to 33, respectively. This indicates that the interlayer space of kaolinite has a limited sorption capacity probably originating from the lack of a permanent negative charge in a region that is normally inaccessible to ions that might cause isomorphous substitution, necessary to yield a permanent charge.

## 6. Conclusions

The following main conclusions can be obtained from the results of this study:

- Clinoptilolite showed much higher sorption capacity toward  $\text{Cs}^+$  ions than kaolinite.
- The sorption of  $\text{Cs}^+$  on kaolinite and clinoptilolite might be described by second-order kinetics, with the rate constants indicating faster sorption on kaolinite, which also possesses a lower activation energy barrier toward  $\text{Cs}^+$  fixation.
- Pore diffusion seems to be effective in the uptake steps of  $\text{Cs}^+$  by clinoptilolite.

- The sorption data on both minerals is well described by Freundlich and Dubinin–Radushkevich isotherm models.
- The uptake of Cs<sup>+</sup> on both minerals is exothermic and spontaneous with energy values corresponding to electrostatic type interactions (ion exchange).
- The lattices of both minerals seems to be unaffected by the sorption of Cs<sup>+</sup> ions.
- Expanding the interlayer space of kaolinite using DMSO did not yield a significant increase in the amount of retarded Cs<sup>+</sup>.
- The EDS findings revealed no localization in the sorbed Cs<sup>+</sup> on the surfaces of both minerals and demonstrated the higher fixation ability of clinoptilolite.

### Acknowledgments

This research was sponsored by the fund 2003 IYTE 04. The authors thank Mr. Sinan Yılmaz for his help with the AAS measurements, and the Center of Material Research, Izmir Institute of Technology, for their assistance in the SEM/EDS and XRPD measurements.

### References

- [1] K.H. Lieser, *Radiochim. Acta* 70/71 (1995) 355.
- [2] J.I. Drever, *The Geochemistry of Natural Waters*, Prentice–Hall, Englewood Cliffs, NJ, 1982.
- [3] F. Coppin, G. Berger, A. Bauer, S. Castet, M. Loubet, *Chem. Geol.* 182 (2002) 57.
- [4] C. Ma, R.A. Eggleton, *Clays Clay Miner.* 47 (1999) 174.
- [5] M.D.A. Bolland, A.M. Posner, J.P. Quirk, *Clays Clay Miner.* 28 (1980) 412.
- [6] J. Perić, M. Trgo, N.V. Medvidović, *Water Res.* 381 (2004) 1893.
- [7] W. Mozgawa, *J. Mol. Struct.* 596 (2001) 129.
- [8] V.J. Inglezakis, M.D. Loizidou, H.P. Grigoropoulou, *J. Colloid Interface Sci.* 261 (2003) 49.
- [9] T. Shahwan, H.N. Erten, *J. Radioanal. Nucl. Chem.* 253 (2002) 115.
- [10] T. Shahwan, H.N. Erten, L. Black, G.C. Allen, *Sci. Total Environ.* 226 (1999) 255.
- [11] J.L. Krumhansl, P.V. Brady, H.L. Anderson, *J. Contam. Hydrol.* 47 (2001) 233.
- [12] C. Willms, Z. Li, L. Allen, C.V. Evans, *Appl. Clay Sci.* 25 (2004) 125.
- [13] Y. Kim, R.T. Cygan, R.J. Kirkpatrick, *Geochim. Cosmochim. Acta* 60 (1996) 1041.
- [14] Y. Kim, R.J. Kirkpatrick, R.T. Cygan, *Geochim. Cosmochim. Acta* 60 (1996) 4059.
- [15] E. Valcke, B. Engels, A. Cremers, *Zeolites* 18 (1997) 205.
- [16] S. Bagosi, L.J. Csetenyi, *Cement Concrete Res.* 29 (1999) 479.
- [17] G.S. Groenewold, R. Avci, C. Karahan, K. Lefebvre, R.V. Fox, M.M. Cortez, A.K. Gianotto, J. Sunner, W.L. Manner, *Anal. Chem.* 76 (2004) 2893.
- [18] J. Chorover, S. Choi, M.K. Amistadi, K.G. Karthikeyan, G. Crosson, K.T. Mueller, *Environ. Sci. Technol.* 37 (2003) 2200.
- [19] R. Patakfalvi, A. Oszko, I. Dekany, *Colloids Surf. A* 220 (2003) 45.
- [20] D. Liu, C. Hsu, C. Chuang, *Appl. Radiat. Isotopes* 46 (1995) 839.
- [21] N. Kannan, M.M. Sundarum, *Dyes Pigments* 51 (2001) 25.
- [22] Y.S. Ho, G. McKay, *Water Res.* 34 (2000) 735.
- [23] A.S. Ozcan, A. Ozcan, *J. Colloid Interface Sci.*, in press.
- [24] F. Helfferich, *Ion Exchange*, McGraw–Hill, New York, 1962.
- [25] J.C. Miranda-Trevino, C.A. Coles, *Appl. Clay Sci.* 23 (2003) 133.